# Ecosystem variability and early human habitats in eastern Africa

Clayton R. Magill[a], Gail M. Ashley[b], and Katherine H. Freeman[a,1]

[a]Department of Geosciences, Pennsylvania State University, University Park, PA 16802; and [b]Department of Earth and Planetary Sciences, Rutgers University, Piscataway, NJ 08854

This Feature Article is part of a series identified by the Editorial Board as reporting findings of exceptional significance.

Edited by John M. Hayes, Woods Hole Oceanographic Institution, Berkeley, CA, and approved November 12, 2012 (received for review April 25, 2012)

**The role of savannas during the course of early human evolution has been debated for nearly a century, in part because of difficulties in characterizing local ecosystems from fossil and sediment records. Here, we present high-resolution lipid biomarker and isotopic signatures for organic matter preserved in lake sediments at Olduvai Gorge during a key juncture in human evolution about 2.0 Ma—the emergence and dispersal of *Homo erectus* (sensu lato). Using published data for modern plants and soils, we construct a framework for ecological interpretations of stable carbon-isotope compositions (expressed as $\delta^{13}C$ values) of lipid biomarkers from ancient plants. Within this framework, $\delta^{13}C$ values for sedimentary leaf lipids and total organic carbon from Olduvai Gorge indicate recurrent ecosystem variations, where open $C_4$ grasslands abruptly transitioned to closed $C_3$ forests within several hundreds to thousands of years. Carbon-isotopic signatures correlate most strongly with Earth's orbital geometry (precession), and tropical sea-surface temperatures are significant secondary predictors in partial regression analyses. The scale and pace of repeated ecosystem variations at Olduvai Gorge contrast with long-held views of directional or stepwise aridification and grassland expansion in eastern Africa during the early Pleistocene and provide a local perspective on environmental hypotheses of human evolution.**

climate | plant waxes | hominins | paleovegetation | paleoclimate

Climate-dependent ecosystem characteristics, such as habitat and water availability, likely influenced natural selection during human evolution (1). For example, woody plants may have influenced thermoregulatory and dietary adaptations in hominins and other terrestrial mammals since the Pleistocene (2–4) about 2.6 Ma. Unfortunately, in many cases, reconstructions of ecosystem characteristics and climate at hominin archaeological sites are limited by poor preservation and coarse temporal resolution. Moreover, discontinuities are common in terrestrial sediment sequences. As a result, much of the environmental context of human evolution has been interpreted based on regional and global conditions reconstructed from marine records (5, 6).

The role of savannas in human evolution remains a subject of debate (5–8). This debate stems, in part, from the historically imprecise definition of savanna for modern and ancient ecosystems and the difficulties of estimating plant community compositions—particularly woody cover—from sediments. Recently, the work by Cerling et al. (7) estimated plant community compositions based on present day relationships between woody cover and carbon-isotope compositions for soil carbonates and soil organic matter (SOM). This approach offers insights into ecosystem structures at hominin archaeological sites (e.g., Omo-Turkana Basin), but it is limited to environments supporting ancient soils (paleosols).

Here, we extend the approach in the work by Cerling et al. (7) to include lipid biomarkers archived in lake sediments deposited between about 2.0 and 1.8 Ma at an important hominin archaeological site—Olduvai Gorge. In addition to including key junctures in human evolution (8), this time interval is associated with important changes in tropical climate, including strengthening of east–west (Walker) atmospheric circulation across the Indian and Pacific Oceans (9). Weakened Walker circulation before about 2.0 Ma was similar to conditions projected to accompany the continued rise in greenhouse gas concentrations during the coming century (10). To examine connections among ocean and atmospheric circulation, regional climate, and plant community composition, we also compare our organic carbon signatures to reconstructions of polar ice volume and sea-surface temperatures (SSTs) in the Atlantic and Indian Oceans.

## Background

**Site Descriptions.** Olduvai Gorge is just south of the equator in northern Tanzania (2° 48′S, 35° 06′E), where it cuts across a 50-km rift platform basin to expose a 2.0 million y sequence of lake and river sediments (Fig. 1). The basin formed on the western margin of the East African Rift System in response to extension tectonics and the growth of a large volcanic complex (11, 12). During the early Pleistocene, the basin area covered an estimated 3,500 $km^2$ and included a saline–alkaline lake near its center (12). Sediments from this central lake are composed primarily of reworked volcanic material and air-fall tuffs (11). For our study, we use samples recovered from outcrop exposures near the center of the paleolake that preserve a stratigraphic record of continuous deposition (11).

Today, annual precipitation patterns at Olduvai Gorge and surrounding regions of eastern Africa are defined by monsoon circulation by two major convergence zones (13)—the Intertropical Convergence Zone (ITCZ) and the Interoceanic Confluence (IOC). The ITCZ marks convergence of regional trade winds, whereas the IOC marks zonal confluence of water vapor derived from the Atlantic and Indian Oceans (Fig. 1). Seasonal migrations of the ITCZ and the IOC result in an annual cycle consisting of two rainy seasons separated by arid conditions that last from May to September. Long rains (March to May) produce the largest proportion of total annual precipitation; short rains (October to December) are more variable but also correlate with total annual precipitation (14). Today, Olduvai Gorge experiences mean annual precipitation (MAP) of about 550 mm; several independent proxy archives suggest that MAP ranged between about 400 and 900 mm during the early Pleistocene (15–17).

We compare our data with coeval records for alkenone-derived SSTs from the eastern Atlantic and western Indian Oceans (18–20) (Fig. 1). Ocean Drilling Program (ODP) site 662 (1° 23′S, 11° 44′W, 3,824 m water depth) is in the eastern Atlantic Ocean in the Gulf of Guinea. ODP site 722 (16° 37′N, 59° 48′E, 2,028 m

Author contributions: C.R.M., G.M.A., and K.H.F. designed research; C.R.M. and G.M.A. performed research; C.R.M., G.M.A., and K.H.F. analyzed data; and C.R.M., G.M.A., and K.H.F. wrote the paper.

The authors declare no conflict of interest.

This article is a PNAS Direct Submission.

[1]To whom correspondence should be addressed. E-mail: khf4@psu.edu.

This article contains supporting information online at www.pnas.org/lookup/suppl/doi:10.1073/pnas.1206276110/-/DCSupplemental.

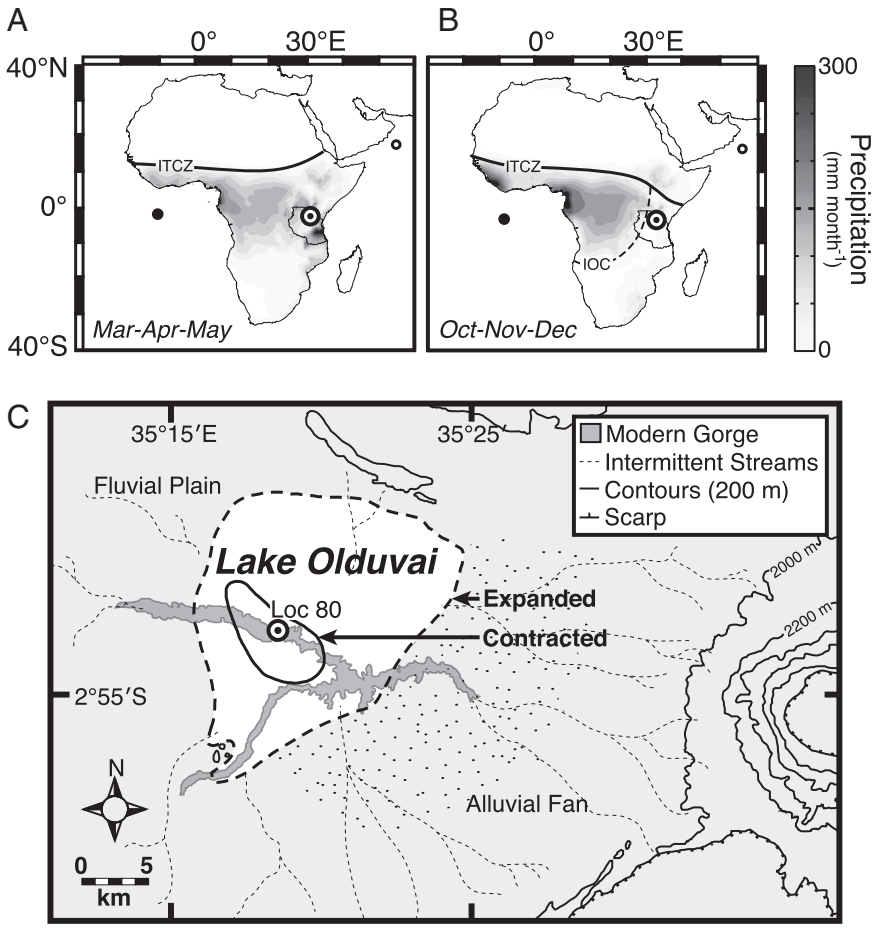


**Fig. 1.** Present day precipitation patterns during long rains (*A*; March to May) and short rains (*B*; October to December) (75). Bold horizontal lines mark the ITCZ. The IOC (*B*; dashed line) is prominent during short rains, and its eastward displacement correlates with higher seasonal precipitation (66). Targets show Olduvai Gorge's location (●, ODP site 662; ○, ODP site 722). (*C*) Depositional environments at Olduvai Gorge during the early Pleistocene about 2.0–1.8 Ma. Expanded and contracted lake levels are reconstructed based on detailed stratigraphic correlations (11, 12, 43).

water depth) is in the northwestern Indian Ocean. Today, SSTs at both sites are sensitive to monsoon-driven seasonal upwelling (21–23), but surface sediment calibrations indicate that alkenone signals reflect mean annual SSTs (22, 23).

**Sedimentary Organic Matter.** Organic matter in lake sediments derives from bacteria, algae, and plants (24), and it integrates contributions from the surrounding watershed (25–28). In contrast, organic matter in soils depends more strongly on local sources and preservation (29, 30), and it can vary spatially over scales of 10 $m^2$ or less (25).

Biomarkers are molecular fossils that have structures with biological specificity (31). Those biomarkers from plants and algae carry isotopic signals derived from terrestrial and aquatic sources, respectively. For instance, long straight-chained hydrocarbons, such as nonacosane ($nC_{29}$) and $nC_{31}$, occur abundantly in leaves (32) and indicate sedimentary inputs from terrestrial plants (33). Although somewhat less specific, certain shorter-chained hydrocarbons (e.g., $nC_{17}$ and $nC_{19}$) indicate contributions from algae and cyanobacteria (31).

**Carbon Isotopes in Leaves, Biomarkers, and Soil Organic Matter.** Photosynthetic carbon-isotopic fractionation is defined between atmospheric carbon dioxide ($\delta^{13}C_{CO2}$) and leaf tissues ($\delta^{13}C_{leaf}$), and its magnitude varies with plant functional type and water availability (34, 35):

$$\varepsilon_{CO2/leaf} = \left[\left(\delta^{13}C_{CO2} + 1{,}000\right)/\left(\delta^{13}C_{leaf} + 1{,}000\right)\right] - 1.$$

We note that $\varepsilon$-values are expressed in permil, which is a unit of parts per thousand. Variability in $\varepsilon_{CO2/leaf}$, which is approximately equivalent to negative $\Delta_{leaf}$ values (widely used in ecological literature) (34), is well-constrained for different photosynthetic pathways (35), but these modern relationships are not easily applied to ancient plants because of limited preservation of leaf tissues through time. Relatively recalcitrant leaf lipids, such as $nC_{31}$, afford an opportunity to circumvent this challenge provided that fractionation between $\delta^{13}C_{leaf}$ and $nC_{31}$ ($\delta^{13}C_{31}$) during biosynthesis can be documented for subtropical and tropical plants (36).

We evaluated carbon-isotopic relationships between soil organic matter ($\delta^{13}C_{SOM}$), leaf tissues, and leaf lipids using published data for 64 plants species and 288 soils from nearly 300 tropical and subtropical localities (Fig. 2). For $C_3$ plant soil systems, we find that $nC_{31}$ is $^{13}C$-depleted by about 7‰ ($n = 45$) with respect to leaf tissue, whereas SOM is $^{13}C$-enriched by about 2‰ ($n = 184$) relative to leaves. Thus, in $C_3$ ecosystems, there is an isotopic difference ($\varepsilon_{SOM/31}$) between $nC_{31}$ and SOM equal to about 9‰:

$$\varepsilon_{SOM/31} = \left[\left(\delta^{13}C_{SOM} + 1{,}000\right)/\left(\delta^{13}C_{31} + 1{,}000\right)\right] - 1.$$

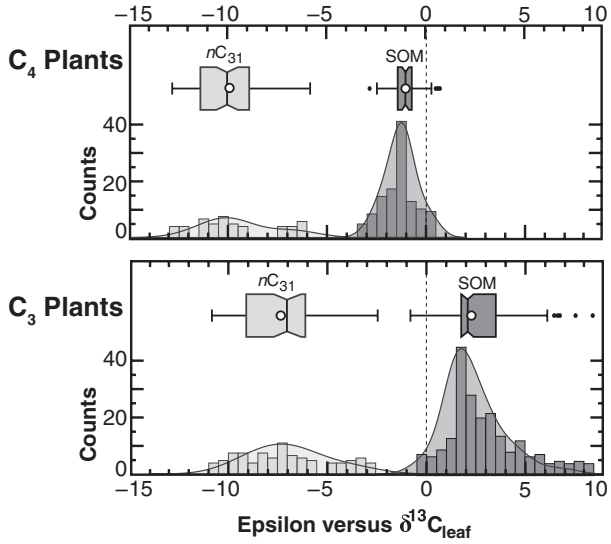


**Fig. 2.** Histograms and box-and-whisker plots for $\varepsilon_{SOM/31}$ from published $\delta^{13}C_{SOM}$ and $\delta^{13}C_{31}$ values from subtropical and tropical regions (*SI Appendix*). Published data are binned at 0.5‰ intervals (counts) based on site averages. Values for $\delta^{13}C_{SOM}$ (dark gray) and $\delta^{13}C_{31}$ (light gray) are plotted relative to $\delta^{13}C_{leaf}$. Values of $\varepsilon_{SOM/31}$ equal about 9‰ in both $C_3$ and $C_4$ ecosystems. Individual boxes contain interquartile ranges (IQRs). Bold vertical lines within boxes mark median values. ○, mean values. Horizontal whiskers mark minimum and maximum values, except values outside of 1.5 IQR (●). Notch half-width values indicate confidence in differentiating median values.

In $C_4$ plant soil systems, both $nC_{31}$ and SOM are $^{13}C$-depleted with respect to leaf tissue by about 10‰ ($n = 19$) and 1‰ ($n = 104$), respectively. Accordingly, $\varepsilon_{SOM/31}$ in $C_4$ ecosystems also equals about 9‰. Therefore, we apply $\varepsilon_{SOM/31}$ of 9‰ to estimate $\delta^{13}C_{SOM}$ from $\delta^{13}C_{31}$ values, thus extending to plant waxes the predictive capabilities of $\delta^{13}C_{SOM}$ for estimating woody cover (7) (Fig. 3). We caution that the value of 9‰ for $\varepsilon_{SOM/31}$ derived here is based on data from xeric woodlands and scrublands, tropical deciduous forests, and $C_4$ grasslands, and it may not be representative for other ecosystems (36).

The fractional abundance of $C_3$ plants is inversely related to $C_4$ plants in tropical ecosystems (25, 37). However, the relationship between woody cover ($f_{woody}$) and $C_4$ abundance is nonlinear (7), because herbaceous $C_3$ plants can occur in both open and wooded ecosystems (38). As a result, for $\delta^{13}C_{SOM}$ values between near-total $C_3$ composition (−30‰) and negligible $C_3$ cover (−14‰), we follow the approach in the work by Cerling et al. (7) to estimate $f_{woody}$ (where $-13 \le \delta^{13}C_{SOM} \ge -31‰$):

$$f_{woody} = \left(\sin\left(-1.06688 - 0.08538\ \delta^{13}C_{SOM}\right)\right)^2.$$

**Structural Classification for Ancient Ecosystems.** The broad functional definition for savannas as a continuous herbaceous understory with irregular distributions of trees or bushes does not account for differences in $f_{woody}$ (39). Therefore, we adopt definitions for African plant communities defined by the United Nations Educational, Scientific and Cultural Organization (UNESCO) (40). According to this classification scheme, (*i*) forests display continuous tree cover (>10 m) with interlocking crowns and poorly developed understory, (*ii*) woodlands—including bush/shrublands—display open or closed stands of shrubs or trees (up to 8 m) with at least 40% woody plant cover and understory with grasses and other herbs, (*iii*) wooded grasslands display 10–40% woody plant cover and well-developed groundcover with grasses and other herbs, (*iv*) grasslands display less than 10% woody plant cover and well-developed groundcover with grasses and other herbs, and (*v*) deserts display sparse groundcover and sandy, stony, or rocky substrate. UNESCO does not distinguish between forests and woodlands in terms of woody plant cover, but here, we consider forests to display greater than 80% woody plant cover (7, 39).

The evolutionary implications of orbital forcing on environmental change were recognized over a century ago (41) but remain controversial today (3–6). Marine sediments just off African

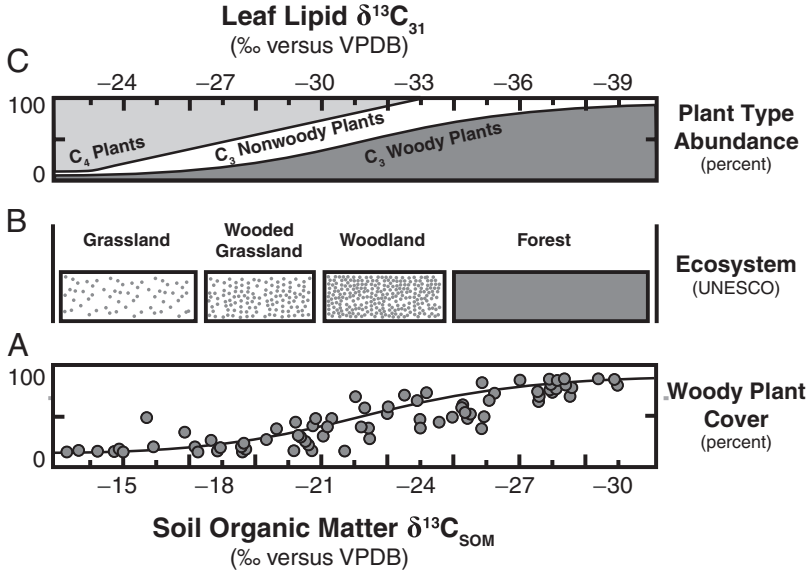


**Fig. 3.** Stable carbon-isotope compositions for SOM ($\delta^{13}C_{SOM}$; bottom *x* axis) and $nC_{31}$ ($\delta^{13}C_{31}$; top *x* axis) relative to woody plant cover (*A*), ecosystem (*B*), and plant community composition (*C*). The published relationship between woody plant cover and $\delta^{13}C_{SOM}$ is described by the following function, where $-13 \le \delta^{13}C_{SOM} \ge -31‰$ (10): $f_{woody} = (\sin(-1.06688 - 0.08538\ \delta^{13}C_{SOM}))^2$. Here, we relate $\delta^{13}C_{SOM}$ to $\delta^{13}C_{31}$ using a value of 9‰ for $\varepsilon_{SOM/31}$. The relationship between woody plant cover and $\delta^{13}C_{31}$ is, thus, described by the following function, where $-22 \le \delta^{13}C_{SOM} \ge -40‰$): $f_{woody} = (\sin(-1.83530 - 0.08538\ \delta^{13}C_{31}))^2$. Ecosystem definitions adhere to African plant communities according to UNESCO terminology (40).

shores document orbital rhythms in terrestrial inputs during the Pleistocene (5), and a growing number of terrestrial sequences hint at a similar pacing for environmental changes in eastern Africa (42, 43). Marine sequences are often indirectly or too poorly constrained in time to infer relationships between key junctures in human evolution and terrestrial conditions or change (6). Lithostratigraphic patterns in lake margin sediments at Olduvai Gorge reveal five episodes of lake expansion between *ca.* 1.85 and 1.74 Ma, suggesting that lake level changes may have tracked orbital precession (43). Here, we use sedimentary organic matter signatures in high-resolution and temporally well-constrained lake sediments to evaluate the magnitude and timing of ecosystem changes associated with lake level changes.

## Results and Discussion

**Ecosystem Change and Woody Cover.** We observe repeated shifts in $\delta^{13}C_{31}$ values between about −36‰ and −20‰ (Fig. 4), which track closely with orbitally paced lake margin lithostratigraphic patterns, suggesting that ecosystem changes at Olduvai Gorge were also influenced by orbital cycles (Fig. 5). Total organic carbon (TOC) $\delta^{13}C$ values ($\delta^{13}C_{TOC}$) show a smaller isotopic range of about 9‰ and correlate tightly with $\delta^{13}C_{31}$ values ($r^2$ = 0.86); $\delta^{13}C_{TOC}$ values follow terrestrial plant inputs but are attenuated, likely by algal or macrophytic inputs. Taken together, $\delta^{13}C_{31}$ and $\delta^{13}C_{TOC}$ values suggest rapid local ecosystem shifts between closed $C_3$ woodlands and open $C_4$ grasslands. These changes were comparable with extreme events, such as the greening of the Sahara about 120,000 y ago, that accompanied the dispersal of modern humans out of Africa (44).

Carbon-isotope evidence for pronounced ecosystem shifts at Olduvai Gorge contrasts with previous reconstructions for eastern Africa that proposed that ecosystems were stable at local to regional scales in the early Pleistocene (15, 45, 46) and generally lacked closed woodlands near hominin archaeological sites since 6 Ma (7). Dramatic and rapid changes in $\delta^{13}C_{31}$ values highlight ecosystem instability in this region; furthermore, $\delta^{13}C_{31}$ values indicate that closed woodlands dominated local landscapes for up to 20% of the time.

Differences in the interpretation of ancient ecosystems, in addition to problems related to savanna heterogeneity, can stem from inherent proxy biases (6). For instance, $\delta^{13}C_{SOM}$ values can overrepresent $C_4$ inputs as a result of $^{13}C$ enrichment during organic matter decomposition (47). Values for $\delta^{13}C_{31}$ can also overrepresent $C_4$ inputs as a result of inorganic carbon (e.g., bicarbonate) assimilation by macrophytes, although $\delta^{13}C_{31}$ values in arid environments are more likely biased to wet conditions (when plants synthesize most leaf lipids) (48). Although specific mechanisms responsible for differences among ecosystem proxies cannot necessarily be reconciled here, we suggest that carbon-isotopic signals for leaf lipids can complement $\delta^{13}C_{SOM}$ values, which otherwise can skew to $C_4$—and thus, arid—signals on seasonal and longer timescales.

**Biogeochemical Variability at the Ecosystem Scale.** Organic matter in lake sediments incorporates inputs from both aquatic and terrestrial photosynthetic organisms and can vary in proportion with productivity and deposition in a lake and the surrounding watershed. At Olduvai Gorge, $\delta^{13}C_{TOC}$ values correlate strongly with TOC (%TOC; $r^2$ = 0.84) but show no clear relationship with algal vs. terrestrial plant inputs (Fig. 4):

$$P_{alg} = (nC_{17} + nC_{19})/(nC_{17} + nC_{19} + nC_{29} + nC_{31}).$$

The abundance ratio of pristane vs. phytane is constantly near 2.5, suggesting that organic carbon deposition was dominated by terrestrial plant input (31). These observations corroborate strong

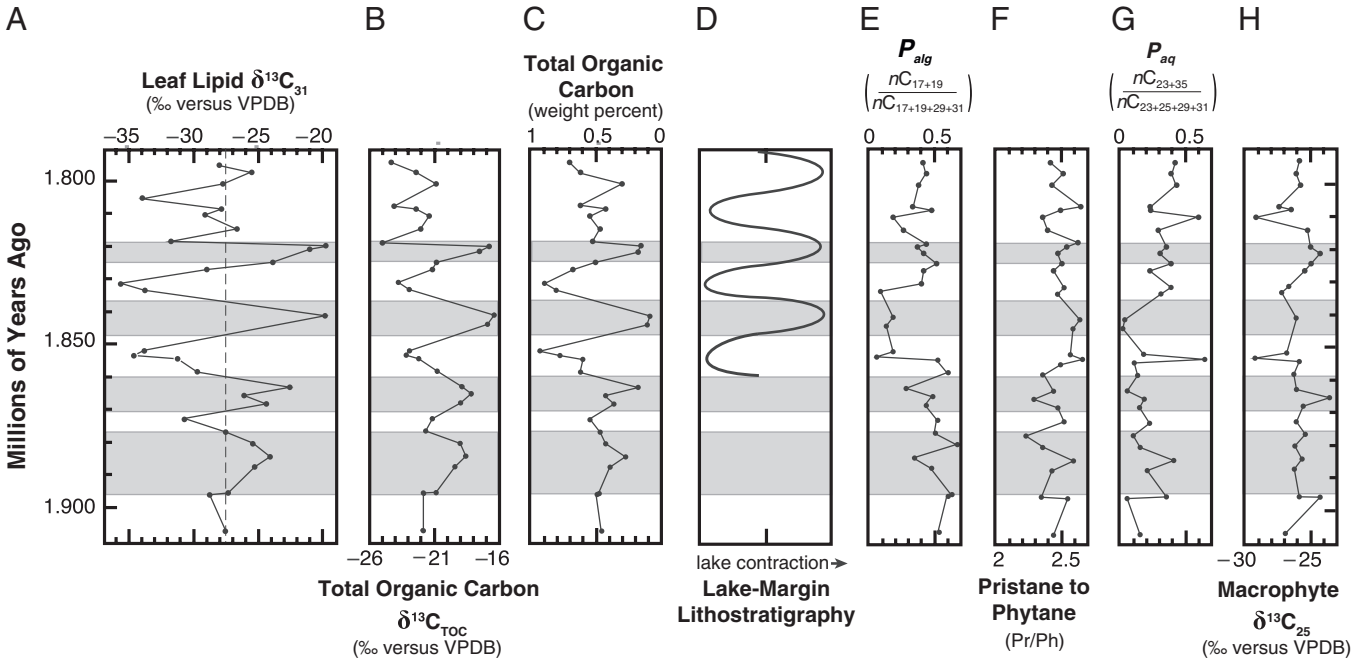


**Fig. 4.** Biomarker and isotopic signatures for organic matter preserved in lake sediments at Olduvai Gorge. (*A*) Leaf lipid $\delta^{13}C$ values for $nC_{31}$ ($\delta^{13}C_{31}$). (*B*) TOC $\delta^{13}C$ values ($\delta^{13}C_{TOC}$). (*C*) TOC percentages (%TOC). (*D*) Diagrammatic depiction of relative lake level changes at Olduvai Gorge based on lake margin lithostratigraphy (43). (*E*) Ratios of algal lipids ($nC_{17} + nC_{19}$) relative to algal and terrestrial plant lipids ($nC_{17} + nC_{19} + nC_{29} + nC_{31}$). Higher values reflect relatively increased algal inputs (31). (*F*) Ratios of pristane (Pr) to phytane (Ph). In lake sediments, values above two generally reflect a dominance of terrestrial plant inputs (31). (*G*) Ratios of macrophytic lipids ($nC_{23} + nC_{25}$) relative to macrophytic and terrestrial plant lipids ($nC_{23} + nC_{25} + nC_{29} + nC_{31}$; that is, $P_{aq}$). Higher values reflect relatively increased macrophytic inputs (50). (*H*) Values of $\delta^{13}C$ for the macrophytic lipid $nC_{25}$ ($\delta^{13}C_{25}$). Horizontal gray bands highlight periods of time characterized by $\delta^{13}C_{31}$ values higher than about −28‰ (i.e., open grassland and wooded grassland ecosystems).

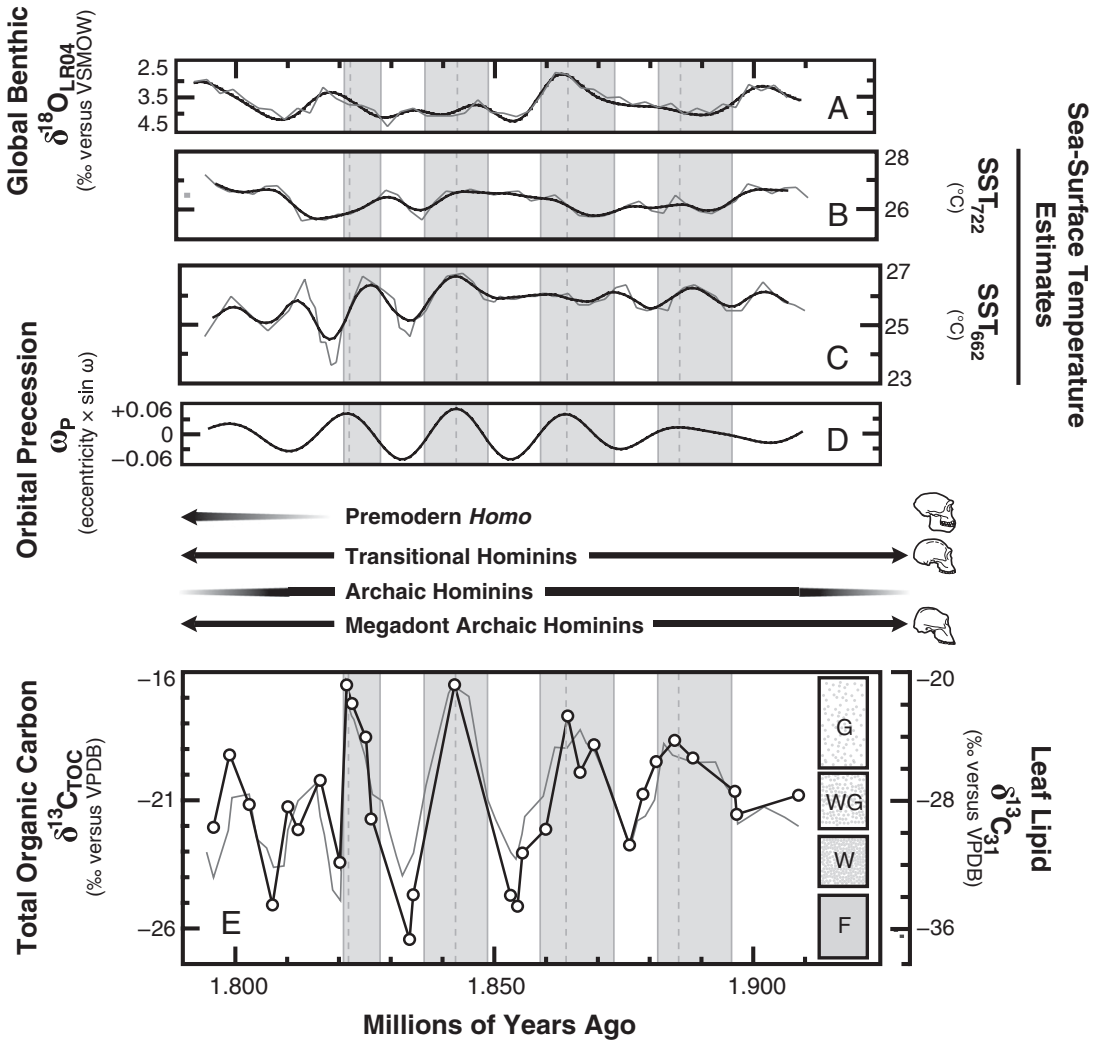


**Fig. 5.** Time series for global, regional, and local proxy indicators during the early Pleistocene. (*A*) Global benthic oxygen-isotopic composite (19). Gray lines connect original data, and the bold black line shows a five-point smoothing. (*B* and *C*) Alkenone-derived SST estimates for the western Indian Ocean ($SST_{722}$) and eastern Atlantic Ocean ($SST_{662}$), respectively (18–20). Gray lines connect original data, and bold black lines show five-point smoothing. (*D*) Calculated orbital precession ($\omega_p$). Values for $\omega_p$ equal the product of calculated eccentricity (*e*) and the sine function of the longitude of the perihelion ($\omega$). (*E*) Leaf lipid $\delta^{13}C$ values for $nC_{31}$ ($\delta^{13}C_{31}$; ○ connected by bold black lines) and TOC $\delta^{13}C$ values ($\delta^{13}C_{TOC}$; gray lines). F, forest; G, grassland; W, bush/shrubland and woodland; WG, wooded grassland. Ecosystem definitions adhere to African plant communities according to UNESCO terminology (40) based on $\delta^{13}C_{31}$ values (Fig. 4). Vertical gray bands highlight periods of time characterized by $\delta^{13}C_{31}$ values higher than about −28‰ (i.e., open grassland and wooded grassland ecosystems). Hominin taxonomic grades and fossil occurrences are illustrated using information in the work by Wood (76); skulls denote taxonomic grades that have been identified at Olduvai Gorge.

correlation between $\delta^{13}C_{TOC}$ and $\delta^{13}C_{31}$ values and suggest that $\delta^{13}C_{TOC}$ values primarily follow terrestrial plant inputs.

Macrophytes contain abundant intermediate-chain *n*-alkanes (e.g., $nC_{23}$ and $nC_{25}$) but limited long-chain homologs compared with most terrestrial plants (49, 50). Thus, relative abundances of $nC_{23}$ and $nC_{25}$ vs. $nC_{29}$ and $nC_{31}$ (that is, $P_{aq}$) can provide estimates for macrophytic vs. terrestrial plant inputs (50):

$$P_{aq} = (nC_{23} + nC_{25})/(nC_{23} + nC_{25} + nC_{29} + nC_{31}).$$

In lake sediments from Olduvai Gorge, $\delta^{13}C_{31}$ values correlate weakly with both $P_{aq}$ ($r^2 = 0.17$) and $nC_{25}$ $\delta^{13}C$ values ($r^2 = 0.19$), suggesting that macrophytes did not significantly contribute to $nC_{31}$ inputs. $P_{aq}$ and $P_{alg}$ are measures of relative abundance of molecules. They do not directly indicate a proportion of biomass from different organisms; instead, these ratios are useful for identifying organic facies or correlations with other biogeochemical signals.

**Mechanisms of Ecosystem Change.** Atmospheric $CO_2$ concentrations ($pCO_2$), temperature, seasonality, and water availability are potential determinants of $C_3$ vs. $C_4$ plant abundance (38). Since the middle Pleistocene, records of $pCO_2$ correlate strongly with polar ice volume changes (51, 52), which were obliquity paced before ~1 Ma (5). Lake sediment $\delta^{13}C_{TOC}$ values for Olduvai Gorge correlate weakly with reconstructed polar ice volumes ($r^2 = 0.16$) based on marine oxygen-isotopic records (9, 19), suggesting that ecosystem changes in this region did not track 41,000-y glacial cycles. If polar ice volume is a representative proxy for $pCO_2$ during the early Pleistocene, then local ecosystem changes were not exclusively tied to $pCO_2$ changes. This conclusion contrasts with suggestions of a dominant role for $pCO_2$ in southern African ecosystems during the early Pleistocene based on speleothem carbonate $\delta^{13}C$ values (53), but it is in agreement with marine oxygen-isotopic evidence for eastern African climate sensitivity to polar ice volume only after 1.0 Ma (54). Values for $\delta^{13}C_{TOC}$ correlate strongly with precession ($\omega_p$) and thus, do not support

temperature as primary determinant of ecosystem change, because $\omega_p$ negligibly influences mean annual temperatures (55). Similarly, paleosol carbonates indicate that mean annual temperatures varied by less than about ±5 °C at and around Olduvai Gorge during the early Pleistocene (56, 57). Strong correlation between $\delta^{13}C_{TOC}$ and $\omega_p$ also suggests that biotic (e.g., herbivory) or abiotic disturbances, such as fire, were not primary determinants of ecosystem change, although they may have served as feedback mechanisms that accelerated changes. In agreement with a variety of other studies (58, 59), we suggest that changing $C_3$ and $C_4$ plant abundances at Olduvai Gorge varied with orbital precession in response to water availability.

**Mechanisms of Hydroclimate Change.** Cycles of about 21,000 y are common in a variety of hydroclimate proxy records in eastern Africa since the Pliocene (5), and $\delta^{13}C_{TOC}$ values correlate strongly with $\omega_p$ ($r^2 = 0.61$) in single-factor regression (*SI Appendix*). Although specific mechanisms responsible for these cycles remain unclear, the timing and magnitude of local and regional hydroclimate changes are consistent with theoretical effects of $\omega_p$ on monsoon strength (60) (that is, higher summer insolation would enhance land–ocean temperatures contrasts, resulting in stronger monsoons and increased precipitation).

Insolation alone cannot account for the magnitude of hydroclimate change in eastern Africa (61). Previous reconstructions based on pollen and oxygen-isotope compositions of soil carbonates suggest that MAP fluctuated between ~400 and 800 mm at Olduvai Gorge and surrounding regions during the early Pleistocene (15–17, 43). However, in climate simulations, insolation variability accounts for MAP fluctuations of less than 200 mm and mostly affects long rains (60, 61). Thus, precipitation amounts in the past must have been impacted by multiple factors, the same as they are today (13).

Today, precipitation in eastern Africa responds sensitively to SSTs in the Indian Ocean and Atlantic Ocean (62). In particular, intensifications of short rains (up to 200 mm) accompany coordinated warm and cold SST anomalies in the western Indian Ocean and eastern Atlantic Ocean (63–65), respectively, as a result of transcontinental surface pressure gradients across Africa and monsoon displacement of the IOC from west to east (66). Partial regressions reveal that SSTs for ODP sites 662 ($SST_{662}$) and 722 ($SST_{722}$) are significant ($P < 0.001$) secondary predictors that are statistically independent of covariance with $\omega_p$, and the combination of $\omega_p$, $SST_{662}$, and $SST_{722}$ explains 73% of the variability in $\delta^{13}C_{TOC}$ values in a multiple regression model. During the early Pleistocene, both $SST_{662}$ and $SST_{722}$ show strong $\omega_p$ and 41,000-y (obliquity) periodicity (20), but only $SST_{662}$ shows a consistent relationship with monsoon-driven upwelling (20). Because upwelling in the eastern Atlantic correlates positively with monsoon strength during late boreal summer (20–22), we suggest that obliquity-paced cooling in the eastern Atlantic Ocean and monsoon strengthening (and therefore, stronger westerly winds) resulted in more frequent eastward displacements of the IOC and intensification of short rains in eastern Africa.

**Ecosystems and Hominin Evolution.** Fossil evidence for pronounced aridification and faunal turnover in eastern Africa between about 2.0 and 1.8 Ma has sparked hypotheses linking the emergence and dispersal of the genus *Homo* to climate-driven ecosystem change (2–6). Fossil evidence for cranial expansion in premodern *Homo* (e.g., *H. erectus* sensu lato) has been linked to irregular resource distributions (67), and our carbon-isotopic data are consistent with enhanced ecosystem variability as a context for encephalization (Fig. 5). During the early Pleistocene, strong ecosystem preferences are not apparent between transitional (e.g., *H. habilis*) and archaic (e.g., *Paranthropus boisei*) hominins (68); however, isotopic and fossil data suggest that transitional species accessed a broad spectrum of dietary resources compared with archaic species (68–70). Among primates, quality (i.e., energy density) of dietary resources correlates strongly with brain size (67). Assuming that dietary resources were primarily unrelated to technological innovations by transitional species (4, 68), we hypothesize that ecosystem variability favored hominin species with large brains that allowed for versatile foraging strategies and dietary diversity.

## Conclusions

This study presents high-resolution biomarker and $\delta^{13}C$ records of ecosystem variability from lake sediments at Olduvai Gorge that were deposited during an interval of pronounced shifts in vertebrate community and global climate reorganization about 2.0–1.8 Ma. Values of $\delta^{13}C_{31}$ indicate rapid and repeated ecosystem restructuring between closed $C_3$ woodlands and open $C_4$-dominated grasslands. Our $\delta^{13}C$ records reveal coupled fluctuations between ecosystem and precession. Additional variability is explained by differences in SST between the Atlantic and Indian Oceans. These observations suggest aridity-controlled, as opposed to carbon dioxide- or temperature-controlled, woody plant cover in eastern Africa during the early Pleistocene. We conclude that highly variable ecosystems accompanied the emergence and dispersal of the genus *Homo*. Our study also builds on soil data to construct an interpretive framework for ecosystem reconstruction based on leaf lipids.

## Materials and Methods

**Reconstructions for Polar Ice Volume.** We use the approach in the work by Bintanja and van de Wal (71), which assumes that a global composite record of benthic $\delta^{18}O$ values (LR04 Stack) accurately traces polar ice volume during the early Pleistocene (19).

**Multiple Regression Analysis.** We used rank transformation (72) and Fourier cross-correlation (73) to compare nonlinear, time-shifted, and unevenly sampled proxy records (*SI Appendix*). Because $\omega_p$ correlates most strongly with $\delta^{13}C_{TOC}$ in single-factor analyses ($r^2 = 0.61$), we constrain multiple regression models for $\delta^{13}C_{TOC}$ values to always include $\omega_p$. This approach is justified, because the influence of $\omega_p$ on climate in eastern Africa is well-supported by theory and other observations (10, 61). Because $\omega_p$ is correlated with other factors, care is required in evaluating additional influences on $\delta^{13}C_{TOC}$ values. We assessed the influence of other factors on $\delta^{13}C_{TOC}$ values using multivariate partial regression models that account for covariance between $\omega_p$ and other factors. Partial regression models with $SST_{662}$ (partial $r^2 = 0.17$) and $SST_{722}$ (partial $r^2 = 0.11$) as secondary predictors are the only models with notable explanatory power for $\delta^{13}C_{TOC}$ values. The following equation shows the $\delta^{13}C_{TOC}$ relationship shared with $\omega_p$, $SST_{662}$, and $SST_{722}$ ($r^2 = 0.73$):

$$\delta^{13}C_{TOC} = 34.7(\pm 2.9)\omega_p + 1.4(\pm 0.1)SST_{662} - 1.4(\pm 0.2)SST_{722} - 20.6(\pm 6.8).$$

**Lipid Extraction and Purification.** Freeze-dried and ground lake sediments were Soxhlet-extracted with dichloromethane:methanol (9:1 vol/vol) for 12 h. Total lipid extracts were then separated into apolar and polar fractions over alumina with hexanes and methanol, respectively. Apolar molecules were separated into saturated and unsaturated fractions over 5% (wt/wt) silver nitrate-impregnated alumina with hexanes and dichloromethane, respectively. Finally, unsaturated apolar compounds were separated with a 5-Å molecular sieve to isolate *n*-alkanes.

**Isotopic Analysis.** All $\delta^{13}C_{TOC}$ values were measured after decarbonation of ground lake sediments with excess 2N hydrochloric acid (74). Residual materials were combusted in an elemental analyzer, and $\delta^{13}C_{TOC}$ values were measured in a ThermoFinnigan Delta+ XP. Standard reference materials of known $\delta^{13}C$ values, including polyethylene foil (NIST 8540), were used throughout sample runs to ensure accuracy. SD (1σ) for NIST 8540 equaled 0.1‰.

Compound-specific $\delta^{13}C$ values were measured by GC–isotope ratio monitoring–MS (Delta+ XP; ThermoFinnigan) with a combustion interface. Carbon dioxide gas of known $\delta^{13}C$ value was used as an external standard; internal standards (i.e., $nC_{41}$, androstane, and squalane; Schimmelmann Standards) were used throughout sample runs to ensure accuracy. SD (1σ) equaled 0.3‰.

**ACKNOWLEDGMENTS.** We are grateful to Richard Hay (1926–2006), whose pioneering work at Olduvai Gorge inspired this research. We thank the Winston Churchill Foundation, Carbon Educators and Researchers Together for Humanity (CarbonEARTH) (National Science Foundation Grant Division of Graduate Education 0947962), and the Tanzania Antiquities Department. We also thank the Ngorongoro Conservation Area Authority for field permits to R. Blumenschine and F. Masao. G.M.A. and R. Renaut collected all samples (National Science Foundation Grant Earth Sciences 9903258).

1. Sabeti PC, et al. (2006) Positive natural selection in the human lineage. *Science* 312(5780):1614–1620.
2. Teaford MF, Ungar PS (2000) Diet and the evolution of the earliest human ancestors. *Proc Natl Acad Sci USA* 97(25):13506–13511.
3. Pickering TR, Bunn HT (2007) The endurance running hypothesis and hunting and scavenging in savanna-woodlands. *J Hum Evol* 53(4):434–438.
4. McNabb J (2005) Hominins and the Early-Middle Pleistocene transition: evolution, culture and climate in Africa and Europe. *Geological Society Special Publication* 247: 287–304.
5. deMenocal P (2004) African climate change and faunal evolution during the Pliocene-Pleistocene. *Earth Planet Sci Lett* 220(1-2):3–24.
6. Kingston JD (2007) Shifting adaptive landscapes: Progress and challenges in reconstructing early hominid environments. *Am J Phys Anthropol* 134(Suppl 45): 20–58.
7. Cerling TE, et al. (2011) Woody cover and hominin environments in the past 6 million years. *Nature* 476(7358):51–56.
8. Wood B, Harrison T (2011) The evolutionary context of the first hominins. *Nature* 470(7334):347–352.
9. Ravelo AC, Andreasen DH, Lyle M, Olivarez Lyle A, Wara MW (2004) Regional climate shifts caused by gradual global cooling in the Pliocene epoch. *Nature* 429(6989): 263–267.
10. Haywood AM, et al. (2009) Introduction: Pliocene climate, processes and problems. *Philos Transact A Math Phys Eng Sci* 367:3–17.
11. Hay R (1976) *Geology of the Olduvai Gorge* (University of California Press, Los Angeles).
12. Ashley G, Hay R (2002) Sedimentation patterns in a Plio-Pleistocene volcaniclastic rift-platform basin, Olduvai Gorge, Tanzania. *Sedimentation in Continental Rifts*, eds Renaut R, Ashley G (Society for Sedimentary Geology, Tulsa, OK), pp 107–122.
13. Nicholson S (2000) The nature of rainfall variability over Africa on time scales of decades to millenia. *Global Planet Change* 26(1-3):137–158.
14. Moron V, Robertson A, Ward M, Camberlin P (2007) Spatial coherence of tropical rainfall at the regional scale. *J Clim* 20(21):5244–5263.
15. Bonnefille R, et al. (1995) Glacial/interglacial record from intertropical Africa, high resolution pollen and carbon data at Rusaka, Burundi. *Quat Sci Rev* 14(9):917–936.
16. Sikes NE, Ashley GM (2007) Stable isotopes of pedogenic carbonates as indicators of paleoecology in the Plio-Pleistocene (upper Bed I), western margin of the Olduvai Basin, Tanzania. *J Hum Evol* 53(5):574–594.
17. Bergner A, Trauth M, Bookhagen B (2003) Paleoprecipitation estimates for the Lake Naivasha basin (Kenya) during the last 175 k.y. using a lake-balance model. *Global Planet Change* 36(1-2):117–136.
18. Clemens SC, Murray DW, Prell WL (1996) Nonstationary phase of the Plio-Pleistocene Asian monsoon. *Science* 274(5289):943–948.
19. Lisiecki L, Raymo M (2005) A Plio-Pleistocene stack of 57 globally distributed benthic $^{18}O$ records. *Paleoceanography*, 10.1029/2004PA001071.
20. Cleaveland L, Herbert T (2007) Coherent obliquity band and heterogeneous precession band responses in early Pleistocene tropical sea surface temperatures. *Paleoceanography*, 10.1029/2006PA001370.
21. McIntyre A, Ruddiman W, Karlin K, Mix A (1989) Surface water response of the equatorial Atlantic Ocean to orbital forcing. *Paleoceanography*, 10.1029/PA004i001p00019.
22. Müller P, et al. (1998) Calibration of the alkenone paleotemperature index $U_{37}^{K'}$ based on core-tops from the eastern South Atlantic and the global ocean (60°N–60°S). *Geochim Cosmochim Acta* 62(10):1757–1772.
23. Sonzogni C, et al. (1997) Temperature and salinity effects on alkenone ratios measured in surface sediments from the Indian Ocean. *Quat Res* 47(3):344–355.
24. Mead R, et al. (2005) Sediment and soil organic matter source assessment as revealed by the molecular distribution and carbon isotopic composition of *n*-alkanes. *Org Geochem* 36(3):363–370.
25. Wynn J, Bird M (2008) Environmental controls on the stable carbon isotopic composition of soil organic carbon: Implications for modelling the distribution of $C_3$ and $C_4$ plants, Australia. *Tellus B Chem Phys Meterol* 60(4):604–621.
26. Teisserenc R, et al. (2010) Integrated transfers of terrigenous organic matter to lakes at their watershed level: A combined biomarker and GIS analysis. *Geochim Cosmochim Acta* 74(22):6375–6386.
27. Oline D, Grant M (2002) Scaling patterns of biomass and soil properties: An empirical analysis. *Landsc Ecol* 17(1):13–26.
28. Aleman J, et al. (2012) Reconstructing savanna tree cover from pollen, phytoliths and stable carbon isotopes. *J Veg Sci* 23(1):187–197.
29. Bai E, et al. (2012) Spatial patterns of soil $\delta^{13}C$ reveal grassland-to-woodland successional processes. *Org Geochem* 42(12):1512–1518.
30. Levin N, et al. (2011) Paleosol carbonates from the Omo Group: Isotopic records of local and regional environmental change in East Africa. *Palaeogeogr Palaeoclimatol Palaeoecol* 307(1-4):75–89.
31. Peters K, Walters C, Moldowan J (2005) *The Biomarker Guide* (Cambridge Univ Press, Cambridge, New York).
32. Eglinton G, Hamilton RJ (1967) Leaf epicuticular waxes. *Science* 156(3780): 1322–1335.
33. Freeman K, Colarusso L (2001) Molecular and isotopic records of $C_4$ grassland expansion in the late Miocene. *Geochim Cosmochim Acta* 65(9):1439–1454.
34. Diefendorf AF, Mueller KE, Wing SL, Koch PL, Freeman KH (2010) Global patterns in leaf $^{13}C$ discrimination and implications for studies of past and future climate. *Proc Natl Acad Sci USA* 107(13):5738–5743.
35. Bowling DR, Pataki DE, Randerson JT (2008) Carbon isotopes in terrestrial ecosystem pools and $CO_2$ fluxes. *New Phytol* 178(1):24–40.
36. Diefendorf A, et al. (2011) Production of *n*-alkyl lipids in living plants and implications for the geologic past. *Geochim Cosmochim Acta* 75(23):7472–7485.
37. Lloyd J, et al. (2008) Contributions of woody and herbaceous vegetation to tropical savanna ecosystem productivity: A quasi-global estimate. *Tree Physiol* 28(3): 451–468.
38. Pearcy R, Ehleringer J (1984) Comparative ecophysiology of $C_3$ and $C_4$ plants. *Plant Cell Environ* 7(1):1–13.
39. Ratnam J, et al. (2011) When is a 'forest' a savanna, and why does it matter? *Glob Ecol Biogeogr* 20(5):653–660.
40. White F (1983) *The Vegetation of Africa* (United Nations Scientific and Cultural Organization, Paris).
41. Wallace A (1870) Man and natural selection. *Nature* 3(53):8–9.
42. Deino A, et al. (2006) Precessional forcing of lacustrine sedimentation in the late Cenozoic Chemeron Basin, Central Kenya Rift, and calibration of the Gauss/Matuyama boundary. *Earth Planet Sci Lett* 247(1-2):41–60.
43. Ashley G (2007) Orbital rhythms, monsoons, and playa lake response, Olduvai Basin, equatorial East Africa (*ca.* 1.85–1.74 Ma). *Geology* 35(12):1091–1094.
44. Osborne AH, et al. (2008) A humid corridor across the Sahara for the migration of early modern humans out of Africa 120,000 years ago. *Proc Natl Acad Sci USA* 105(43): 16444–16447.
45. Reed K, Rector A (2007) African Pliocene paleoecology. *Evolution of the Human Diet*, ed Ungar P (Oxford University Press, New York), pp 262–288.
46. Bamford M, et al. (2008) Late Pliocene grassland from Olduvai Gorge, Tanzania. *Palaeogeogr Palaeoclimatol Palaeoecol* 257(3):280–293.
47. Wynn J (2007) Carbon isotope fractionation during decomposition of organic matter in soils and paleosols: Implications for paleoecological interpretations of paleosols. *Palaeogeogr Palaeoclimatol Palaeoecol* 251(3-4):437–448.
48. Post-Beittenmiller D (1996) Biochemistry and molecular biology of wax production in plants. *Annu Rev Plant Physiol Plant Mol Biol* 47(1):405–430.
49. Lamb A, Leng M, Umer Mohammed M, Lamb H (2004) Holocene climate and vegetation change in the Main Ethiopian Rift Valley, inferred from the composition (C/N and $\delta^{13}C$) of lacustrine organic matter. *Quat Sci Rev* 23(7-8):881–891.
50. Ficken K, Li B, Swain D, Eglinton G (2000) An *n*-alkane proxy for the sedimentary input of submerged/floating freshwater aquatic macrophytes. *Org Geochem* 31(7-8): 745–749.
51. Petit J, et al. (1999) Climate and atmospheric history of the past 420,000 years from the Vostok ice core, Antarctica. *Nature* 399(6735):429–436.
52. Lüthi D, et al. (2008) High-resolution carbon dioxide concentration record 650,000–800,000 years before present. *Nature* 453(7193):379–382.
53. Hopley P, et al. (2007) High-and low-latitude orbital forcing of early hominin habitats in South Africa. *Earth Planet Sci Lett* 256(3-4):419–432.
54. Trauth M, Larrasoaña J, Mudelsee M (2009) Trends, rhythms and events in Plio-Pleistocene African climate. *Quat Sci Rev* 28(5-6):399–411.
55. Kingston J (2005) Orbital controls on seasonality. *Seasonality in Primates*, eds Brockman D, van Schaik C (Cambridge University Press, New York), pp 521–543.
56. Hay R, Kyser T (2001) Chemical sedimentology and paleoenvironmental history of Lake Olduvai, a Pliocene lake in northern Tanzania. *Geol Soc Am Bull* 113(12): 1505–1521.
57. Passey BH, Levin NE, Cerling TE, Brown FH, Eiler JM (2010) High-temperature environments of human evolution in East Africa based on bond ordering in paleosol carbonates. *Proc Natl Acad Sci USA* 107(25):11245–11249.
58. Huang Y, et al. (2001) Climate change as the dominant control on glacial-interglacial variations in $C_3$ and $C_4$ plant abundance. *Science* 293(5535):1647–1651.
59. Bobe R (2006) The evolution of arid ecosystems in eastern Africa. *J Arid Environ* 66(3):564–584.
60. Ruddiman W (2001) *Earth's Climate: Past and Future* (Freeman, New York).
61. Clement A, Hall A, Broccoli A (2004) The importance of precessional signals in the tropical climate. *Clim Dyn* 22(4):327–341.
62. Chiang J (2009) The tropics in paleoclimate. *Annu Rev Earth Planet Sci* 37(1):263–297.
63. Vuille M, et al. (2005) Stable isotopes in East African precipitation record Indian Ocean zonal mode. *Geophys Res Lett*, 10.1029/2005JD006022.
64. Balas N, et al. (2007) The relationship of rainfall variability in West Central Africa to sea-surface temperature fluctuations. *Int J Climatol* 27(10):1335–1349.
65. Farnsworth A, et al. (2011) Understanding the large scale driving mechanisms of rainfall variability over Central Africa. *African Climate and Climate Change*, eds Williams C, Kniveton D (Springer, New York), pp 101–122.
66. Eltahir E, Gong C (1996) Dynamics of wet and dry years in West Africa. *J Clim* 9(5): 1030–1042.
67. Snodgrass J, Leonard W, Robertson M (2009) The energetics of encephalization in early hominids. *The Evolution of Hominin Diets*, eds Hublin J, Richards M (Springer, New York), pp 15–29.

68. Wood B, Strait D (2004) Patterns of resource use in early *Homo* and *Paranthropus*. *J Hum Evol* 46(2):119–162.
69. van der Merwe N, Masao F, Bamford M (2008) Isotopic evidence for contrasting diets of early hominins *Homo habilis* and *Australopithecus boisei* of Tanzania. *S Afr J Sci* 104(3-4):153–155.
70. Cerling TE, et al. (2011) Diet of *Paranthropus boisei* in the early Pleistocene of East Africa. *Proc Natl Acad Sci USA* 108(23):9337–9341.
71. Bintanja R, van de Wal RS (2008) North American ice-sheet dynamics and the onset of 100,000-year glacial cycles. *Nature* 454(7206):869–872.
72. Chatfield C (2004) *The Analysis of Time Series* (CRC Press, London).
73. Scargle J (1982) Studies in astronomical time series analysis. Statistical aspects of spectral analysis of unevenly spaced data. *Astrophys J* 263(1):835–853.
74. Brodie CR, et al. (2011) Evidence for bias in C and N concentrations and $\delta^{13}C$ composition of terrestrial and aquatic organic materials due to pre-analysis acid preparation methods. *Chem Geol* 282(3-4):67–83.
75. Mitchell T, Jones P (2005) An improved method of constructing a database of monthly climate observations and associated high resolution grids. *Int J Climatol* 25(6): 693–712.
76. Wood B (2010) Colloquium paper: Reconstructing human evolution: achievements, challenges, and opportunities. *Proc Natl Acad Sci USA* 107(Suppl 2):8902–8909.